The *C. elegans* UNC-23 protein, a member of the BCL-2-associated athanogene (BAG) family of chaperone regulators, interacts with HSP-1 to regulate cell attachment and maintain hypodermal integrity

Poupak Rahmani, Teresa Rogalski, and Donald G Moerman*

Department of Zoology; University of British Columbia; Vancouver, British Columbia, Canada

Mutations in the *unc-23* gene in the free-living nematode, *Caenorhabditis elegans* result in detachment and dystrophy of the anterior body wall musculature and a bent-head phenotype when grown on solid substrate. We have determined that the *unc-23* gene product is the nematode ortholog of the human BAG-2 protein, a member of the Bcl-2 associated athanogene (BAG) family of molecular chaperone regulators. We show that a functional GFP-tagged UNC-23 protein is expressed throughout development in several tissues of the animal, including body wall muscle and hypodermis, and associates with adhesion complexes and attachment structures within these 2 tissues. In humans, the BAG protein family consists of 6 members that all contain a conserved 45 amino acid BAG domain near their C-termini. These proteins bind to and modulate the activity of the ATPase domain of the heat shock cognate protein 70, Hsc70. We have isolated missense mutations in the ATPase domain of the *C. elegans* heat shock 70 protein, HSP-1 that suppress the phenotype exhibited by *unc-23(e25)* mutant hermaphrodites and we show that UNC-23 and HSP-1 interact in a yeast-2-hybrid system. The interaction of UNC-23 with HSP-1 defines a role for HSP-1 function in the maintenance of muscle attachment during development.

Introduction

Mechanical forces play a critical role in morphogenesis, tissue formation and the maintenance of cellular integrity throughout development. An excellent example of the requirement for mechanical force during morphogenesis is the development of the *C. elegans* embryo, which involves the transformation of a round ball of cells into a long thin worm. This transformation entails large-scale cell shape changes, cell spreading and cell migrations, all of which require mechanical forces (for a review see ref. [1]). The requirement for mechanical forces during embryogenesis is not limited to the *C. elegans* embryo. The process of gastrulation, which is common to multicellular embryos, requires mechanical forces that cause some cell layers to fold outwards while others bend and invaginate [2] (for a review see ref. [3]).

Tissue formation also involves mechanical forces. In order to bear different types of mechanical stresses such as tension, compression or shear, tissues produce highly specialized matrices such as skin, bone, and cartilage.[4] Cells are able to control the deposition, composition and maintenance of molecules that make up their surrounding extracellular matrix (ECM), based on the type and magnitude of the mechanical stresses that act on the tissue.[5] Cells under mechanical stress have also been shown to respond by changing the distribution of the structural components that associate with the cytoskeleton and anchoring junctions.[6] The compositions of the biopolymers (i.e. microfilaments, microtubules, and intermediate filaments) that make up the cytoskeleton are tailored to accommodate the mechanical demand that is put on the cell.[7] The ability to rearrange the ECM and the cytoskeleton in the face of mechanical stresses is an essential response, one that allows the cell to maintain its shape and withstand forces that compromise cellular integrity. To keep their shape and maintain their integrity cells within a tissue must be capable of adaptive responses to various types of mechanical stresses.

We are interested in elucidating some of the mechanisms and molecules involved in the maintenance of cell-ECM adhesion in tissues under physiological stress due to muscle attachment and movement. Movement in the free-living nematode *Caenorhabditis elegans* involves transmission of the contractile force of the body wall muscle cells to the cuticle. This transmission is achieved via a continuous physical linkage between the body wall muscle and the cuticle through the basement membrane and hypodermis. Detailed anatomical studies on *C. elegans* have revealed 2 major extracellular matrices that are involved in motility: the basement membrane and the cuticle. The basement membrane is a specialized ECM that covers the pharynx, intestine, gonad, and body wall muscle cells, and is required for myofilament assembly in the body wall muscle.[8,9] The cuticle is required for embryonic morphogenesis, and provides the exoskeleton that covers the outside of the animal (for a review see ref. 10). In between the basement membrane and the cuticle is the hypodermis, which is the nematode's equivalent of skin. The hypodermis not only plays an important role in transmission of force from the muscle to the cuticle, it is also responsible for deposition of the cuticle and perhaps some basement membrane proteins.[8,10,11] Hemidesmosomes, which are the cell-ECM anchoring junctions for the intermediate filaments, are located at both the basal and cuticular membranes of the hypodermis.[8,11] Hemidesmosomes provide the structural and physical linkage between the basement membrane and the cuticle and are therefore direct mediators of muscle to cuticle attachment. The association between the apical and basal hemidesmosomes is made by intermediate filaments, which not only connect the hemidesmosomes but also provide cellular integrity during force transmission .[8] Since the hypodermis is directly involved in the transfer of contractile force from muscle to cuticle, it affords a great opportunity to study the maintenance of cell-ECM attachment during muscle contraction.

To better understand the mechanism involved in the maintenance of adhesion and cellular integrity during mechanical stress, several mutations that affect this pathway have been identified in *C. elegans*.[12,13] These mutations have a very distinct phenotype, which manifests itself in early larval development and involves the progressive detachment of muscle cells from the underlying hypodermis. At least some of the genes defined by this class of mutation appear to be involved in cell-ECM adhesion including *unc-23*,[13] *mua-1, 2, 3, 4, 5, 6, 7, 9, 10, vab-10, let-805, mup-4, ifb-1* and *pat-12*.[12,14-20]

Mutations affecting the *unc-23* gene were first isolated in a forward genetic screen designed to identify animals with visible mutant phenotypes.[21] Among the original 619 mutants that were identified, only Unc-23 mutant animals exhibited a progressive dystrophy of the head musculature resulting in a bent-head phenotype. A detailed analysis of this unique phenotype revealed that mutations in the *unc-23* gene result in loss of hypodermal integrity and detachment of the muscle cells from the hypodermis during larval development in *C. elegans.*[13] These observations suggest that the *unc-23* gene encodes a structural or a regulatory protein that is involved in the maintenance of muscle cell attachment to the hypodermis.

In this paper we describe the identification and characterization of the *unc-23* gene product as the nematode ortholog of the human BAG-2 protein, a member of the Bcl-2 associated athanogene (BAG) family of molecular chaperone regulators. We also provide evidence that the UNC-23 protein interacts with the heat shock cognate protein 70, HSP-1 to maintain intracellular adhesion strength.

Results

The *unc-23* gene encodes a protein with a domain similar to mammalian Bcl-2-associated athanogene 2 (BAG-2), a chaperone regulator.

The *unc-23* gene maps to a region of chromosome V that is uncovered by several deficiencies. We correlated the physical and genetic maps for this region and localized *unc-23* to a region of 12 cosmids defined by the left breakpoint of *mDf1* and the right breakpoint of *sDf71*. Genetic crosses using the *unc-23(e25)* allele and transgenic strains carrying cosmids and fosmids from this region of the genome revealed that *unc-23* resides on the sequenced fosmid H14N18. We have determined that the *unc-23* gene corresponds to the H14N18.1 open reading frame[22] (data available from GenBank/EMBL/ DDBJ under accession #AF068719), by identifying the sequence alterations corresponding to 6 *unc-23* alleles. Two of the mutations identified are deletions of 117 (*ra801*) and 155 (*ra806*) bps and a third mutation (*rh192*) is a 4 bp insertion (**Table 1** and **Fig. 1**). The remaining 3 EMS-induced mutations are GC – AT point mutations. The *unc-23(e25)* allele is a missense mutation that changes the Glu297 codon to a Lys codon. The *e988* and *e324* mutations introduce stop codons into exons 2 and 5, respectively (**Table 1** and **Fig. 1**).

Our sequencing results for the yk293b4 cDNA obtained from the *C. elegans* cDNA project (Y. Kohara, pers. comm.) confirmed the gene structure predicted for the H14N18.1 ORF by the

Table 1. Molecular lesions associated with *unc-23* muations.

Allele	Type of mutation	Residue changes	Exon affected
e25	Missense	GAA (glu) to AAA (lys)	3
e324	Nonsense	CAA (gln) to TAA (stop)	5
e988	Nonsense	CGA (arg) to TGA (stop)	2
ra801	Deletion	117 bp in frame deletion. New Leucine made at site of deletion.	2
ra806	Deletion	155 bp out of frame deletion.	2
rh192	Insertion	GGAA insertion. Frame shift and termination near end of exon	2

Genefinder program.[23] The partial sequences of several other cDNA clones are available at www.wormbase.org, and these data reveal the presence of mRNA species encoding alternative translation start sites (see for example yk1007e10 and yk1745g09). The *unc-23* gene consists of 5 exons (**Fig. 1**) and, based on the cDNA sequence data, can potentially encode 3 different protein isoforms of 458, 457 and 399 amino acids, respectively. A search of the database using the BLAST server at NIH identified a 211 amino acid human protein called BAG-2 with significant sequence similarity to the UNC-23 protein (**Fig. 2**). Human BAG-2 is a member of the Bcl-2 associated athanogene (BAG) family of molecular chaperone regulators.[24]
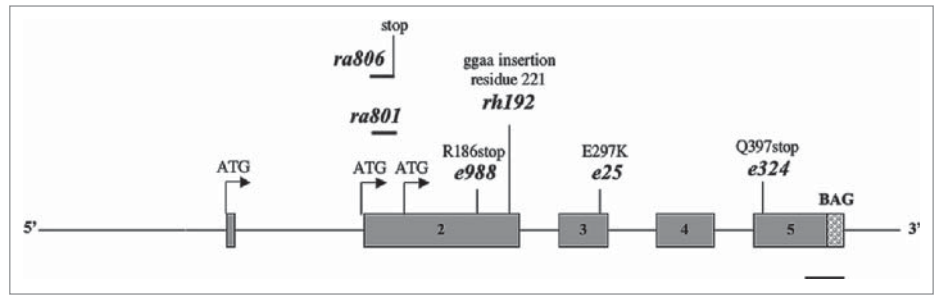

Figure 1. The *unc-23* gene consists of 5 exons and potentially encodes 3 proteins. The intron and exon structure of the *unc-23* gene is shown in the above diagram. Also shown are the locations of the 3 potential start codons identified by cDNA analysis as well as the locations of the alleles that have been identified by sequence analysis. The gene spans 2660 bp from the start codon in exon 1 to the stop codon in exon 5. Scale bar is 150 bp.

The members of this protein family contain a conserved 45 amino acid region, the BAG domain, near their carboxy-termini,
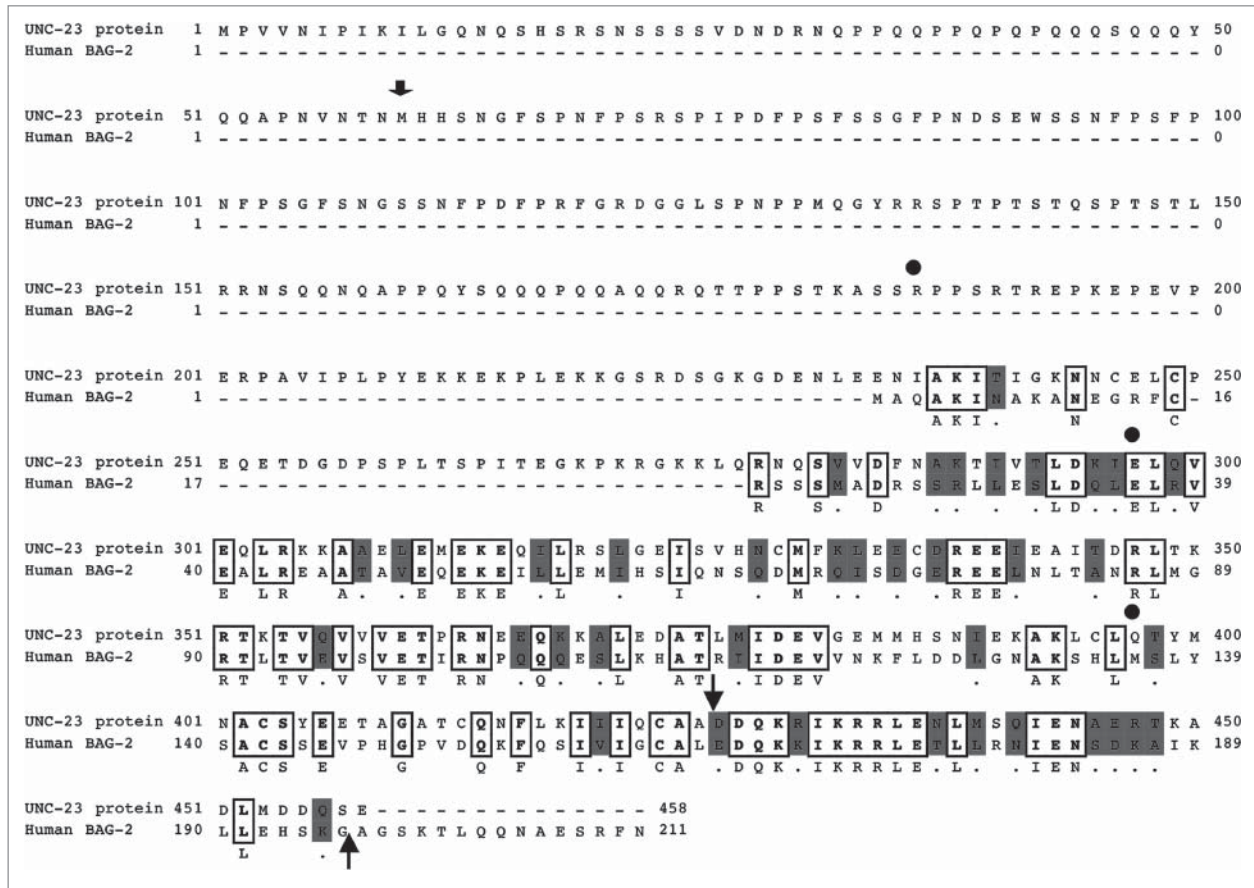

Figure 2. The sequence alignment of UNC-23 and BAG-2 shows homology between the 2 proteins. The human BAG-2 protein is most similar to the carboxy-terminus of the UNC-23 protein. The BAG homology domain of UNC-23 starts at residue 427 and extends to the end of the protein (arrows). The BAG domain in the human BAG-2 protein starts at residue 164 and ends at residue 196. *C. elegans* UNC-23 and human BAG-2 share 40% amino acid identity (shown as boxed residues) and 62% amino acid similarity (highlighted residues) over this region. The N-terminal region of UNC-23 is not homologous to any sequence available in the database and has no predicted structure. The stubby arrow points to the start of the short UNC-23 isoform. The amino acid residues affected by the *e988*, *e324* and *e25* point mutations are indicated by circles. The first 2 mutations introduce stop codons at residues 186 and 397, respectively, and *e25*, the most severe allele of *unc-23*, changes glutamic acid residue 297 to a lysine. This glutamic acid residue is conserved in UNC-23 and BAG-2.

which binds Hsp70/Hsc70 and controls their chaperone activity.[24] To date, 6 members of this family, BAG-1 to BAG-6, have been identified in humans[24,25] and 2 members have been identified in nematodes. The region of similarity between mammalian BAG-2 and UNC-23 is confined to the carboxy-terminus of UNC-23. The amino-terminus of UNC-23 is not similar to any sequence available in the database and has no predicted structure. The BAG domain of UNC-23 starts at residue 427 of the longest protein isoform and extends to the end of the protein (**Fig. 2**). This domain in the human BAG-2 protein starts at residue 164 and ends at residue 196 (**Fig. 2**). *C. elegans* UNC-23 and human BAG-2 share 40% amino acid identity and 62% similarity over the BAG domain and its upstream region.

The UNC-23 protein is present in both body wall muscle and hypodermis.

The *unc-23* gene potentially encodes 3 protein isoforms that differ at their amino-termini. To ensure that the transgene we constructed for microinjection and expression analysis could produce all 3 isoforms as GFP-tagged proteins, we amplified the entire *unc-23* gene, including 2166 bp of promoter, from genomic DNA and inserted the GFP encoding sequences at the 3' end of the gene upstream of the stop codon. All UNC-23 protein

Figure 3. The spatial distribution of a GFP-tagged UNC-23 protein in rescued homozygous *unc-23(e25)* hermaphrodites. The UNC-23::GFP protein is present in a variety of tissues including the hypodermis (**A**) and the body wall muscle cells (**B**) in *unc-23(e25)*V; *raEx20[rol-6; unc-23*::GFP] hermaphrodites. Images are from the mid-section of the animals. Scale bars are 20 microns. (**A**) A view of UNC-23::GFP localization in the hypodermal syncytium is shown. The UNC-23 protein is present throughout the whole of the hypodermis including some, but not all, nuclei and nucleoli. In addition, the GFP-tagged UNC-23 protein is localized in a pattern identical to that seen for intermediate filaments. The closed head white arrow in the hypodermis points to a nucleus that exhibits UNC-23::GFP expression. The open arrow-head arrow points to the in the intermediate filament-like expression pattern. (**B**) A view of UNC-23::GFP localization in 2 body wall muscle cells is shown. The GFP-tagged UNC-23 protein localizes with the dense bodies and M-lines at the cell membrane. The closed head white arrow points to a region of dense bodies and M-lines, while the open arrow-head arrow points to the intermediate filament-like expression pattern in the overlying hypodermis.

isoforms made from this construct will have the GFP attached to their C-terminal. Animals carrying the *raEx20* [*unc-23*::GFP; *rol-6(su1006)*] transgenic array produce at least one functional GFP-tagged UNC-23 protein (shown in **Fig. 3**) that fully rescues the bent-head phenotype of *unc-23(e25)* mutant animals (see **Fig. 4**). GFP fluorescence in animals carrying this array is found throughout development appearing first at the 1.5-fold stage of embryogenesis in a few unidentified cells. Expression of the GFP-tagged UNC-23 protein continues during embryogenesis and by the 3-fold stage, it has expanded to include muscle, hypodermal and pharyngeal cells. In adult hermaphrodites GFP fluorescence is expressed in the pharynx, body wall muscle cells, hypodermis, vulva, and H cells, as well as some unidentified neurons and touch cells. In the hypodermis, UNC-23::GFP is distributed throughout the entire tissue including some nuclei and nucleoli, and in addition, is localized in a pattern reminiscent of the intermediate filaments[8] (shown in **Fig. 3A**). In body wall muscle cells, UNC-23::GFP is localized to the dense bodies and M lines (**Fig. 3B**) in a pattern similar to that observed for several proteins including PAT-3/β-integrin, UNC-112, UNC-97/ PINCH, and PAT-4/ILK.[26-29]

The *unc-23* gene product is required for muscle cell attachment to the hypodermis.

Mutations in the *unc-23* gene result in the progressive detachment of the anterior body wall muscle cells from the hypodermis.[12,13] During embryonic development, muscle cells are capable of myofilament assembly, growth, contraction, and attachment to the hypodermis in the absence of the *unc-23* gene product. However, during mid-larval development body wall muscle cells in the head region of Unc-23 mutant hermaphrodites begin to separate from the hypodermis, resulting in adults with heads that are noticeably thinner than wild type animals. The resulting loss of control of the head causes a bent-head phenotype when the animal tries to move forward. Detachment of the body wall musculature from the hypodermis begins with the anterior-most cells and is usually confined to the head of the animal (compare **Fig. 4A and 4B**). Other phenotypes observed in Unc-23 mutants include the occasional protrusion of the vulva, egg laying defects, mild constipation due to interruption of the defecation cycle and rarely, small blisters at the tip of the nose. The pharynx of Unc-23 mutant animals functions normally. The extent of muscle detachment is highly variable among different mutant strains, ranging from severe to almost wild type (see **Table 2**).

Four of the 6 *unc-23* mutations that have been identified at the sequence level are likely to affect all 3 predicted UNC-23 protein isoforms. The two nonsense mutations should result in either the complete absence of any UNC-23 proteins, or perhaps, the presence of truncated proteins that are missing all, or most of the BAG-2 homologous region of UNC-23. Thus, the severe muscle detachment phenotype exhibited by animals homozygous for these mutations most likely results from the complete absence of *unc-23* gene function. Since hermaphrodites homozygous for the *unc-23(e25)* missense mutation also exhibit a severe phenotype, this mutation is likely to drastically reduce *unc-23* gene function
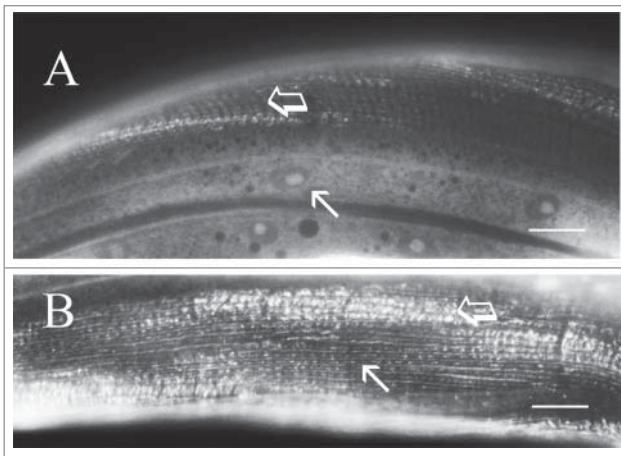
as well. In these mutants, muscle detachments extend just beyond the terminal bulb of the pharynx and involve both the dorsal and ventral quadrants (shown in **Fig. 4B**). The upper tissues completely collapse on top of the pharynx, resulting in complete loss of head movement and a true bent-head phenotype. The GFP-tagged UNC-23 protein(s) produced by the *raEx20* transgenic array completely suppress this muscle detachment phenotype in *unc-23*(*e25*) homozygous hermaphrodites (shown in **Fig. 4C**).

In mutants exhibiting a mild phenotype, the detachments do not extend past the anterior bulb of the pharynx. Only the tip of the nose is affected and, for the most part, no head dragging is observed. The sequence alterations responsible for the mild phenotype exhibited by strains carrying either *unc-23*(*ra801*) or *unc-23*(*ra806*) are known. Neither of these mutations is predicted to result in the complete loss of *unc-23* gene function. The *ra801* mutation is an in frame deletion that eliminates amino acid residues 17 to 55 of the longer protein isoforms, but has no effect on the shortest UNC-23 protein. The *ra806* mutation is an out of frame deletion near the 5' end of the *unc-23* gene that should result in the complete absence of the longer UNC-23 proteins. However, the shortest UNC-23 protein should still be present in animals homozygous for this mutation.

The *e25* missense allele of *unc-23*[21] imparts the most severe phenotype we observed. It is the reference allele of *unc-23* and animals homozygous for *e25* have been used extensively for the characterization and analysis of this gene.[13] A.M.E. Bullerjahn and D. L. Riddle (pers. comm.) observed that *unc-23(e25)*

mutant animals grown in liquid culture fail to exhibit the bent-head phenotype. Suppression of the muscle cell detachment phenotype lasts up to 48 hours after animals are placed on solid medium. Here we have examined the effect of this temporary suppression of muscle detachment on the arrangement of the myofilament lattice and on muscle cell positioning. In liquid grown adult worms, anterior muscle cells are positioned correctly and the myofilaments appear normal when observed under polarized light (shown in **Fig. 4D**). However, these muscle cells are easily detached by mechanical stress. Application of external force, such as putting worms under a coverslip and gently rolling them, can result in the detachment of muscle quadrants from the underlying hypodermis. Subjecting wild-type animals to a similar treatment does not result in any muscle cell detachment. In fact, wild type animals can withstand a great deal more force than the *unc-23(e25)* mutant animals.

The temporary muscle detachment suppression observed with the liquid grown *unc-23(e25)* mutants and the manifestation of this phenotype after transfer to agar plates, suggests there are different forces acting on muscle and hypodermal attachments in these 2 growth conditions.
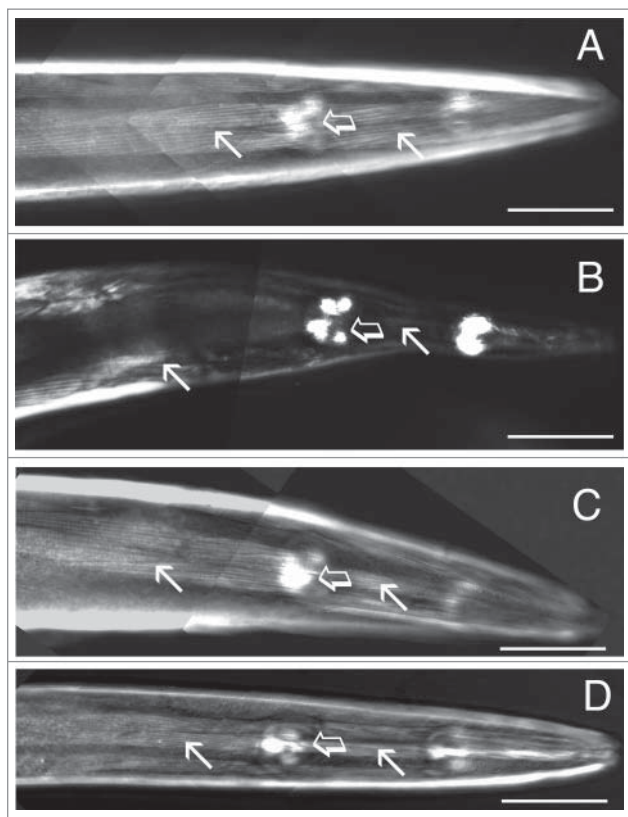

Figure 4. Polarized light images of wild type and *unc-23(e25)* homozygous animals. Polarized light images of a wild type hermaphrodite (**A**), a plate grown homozygous *unc-23(e25)* adult hermaphrodite (**B**), a plate grown *unc-23(e25)*; *raEx20*[*rol-6*; *unc-23*::GFP] hermaphrodite (**C**) and a liquid grown homozygous *unc-23(e25)* adult hermaphrodite (**D**). The closed head white arrows point to regions of muscle birefringence and the open arrow-head arrows point to the terminal bulb of the pharynx. Anterior is to the right in all panels. Scale bars are 60 microns. (**A**) Polarized light image of a wild-type adult hermaphrodite. In *C. elegans,* the body wall muscle cells extend from the tip of the nose to the posterior end of the animal. The myofilament lattice in the muscle sarcomeres is seen as a repeating pattern of light and dark birefringence. The pharynx, which is the grinding apparatus of the worm, can be seen in this image. The bulbous structures are the anterior and posterior bulbs of the pharynx. (**B**) Polarized light image of a plate grown *unc-23(e25)* homozygous adult hermaphrodite. The most anterior muscle cells have detached from the tip of the nose and retracted posteriorly. Note that the head in this animal is thinner than in the wild type animal. The left closed head white arrow point to the region where the muscle cells have stopped detaching and the right closed head white arrow points to a region where the muscle cells have detached. Posterior to the site of detachment, the light and dark pattern of thick and thin filaments can clearly be seen. (**C**) Polarized light image of a plate grown *unc-23(e25)* homozygous adult hermaphrodite carrying the *raEx20* transgenic array. The GFP-tagged UNC-23 protein produced by the transgenic array suppresses the muscle detachment seen in the *unc-23(e25)* homozygous mutant animals. As shown in this image, muscle cells are positioned correctly and extend all the way to the tip of the nose. The light and dark pattern, resulting from the thick and thin filament organization of the myofilament lattice in the sarcomeres, are also well organized and show no defects. (**D**) Polarized light image of an *unc-23(e25)* homozygous animal grown in liquid culture. The muscle quadrants extend to the tip of the nose and no detachment is observed. Animals grown in liquid culture are usually thinner than plate grown animals. The worm shown here is, therefore, thinner than its plate grown counterparts. As shown in this image, muscle cells are positioned correctly and extend all the way to the tip of the nose. The light and dark pattern, resulting from the thick and thin filament organization of the myofilament lattice in the sarcomeres, are also well organized and show no defects.

Table 2. Phenotypes associated with Unc-23 mutant animals.

Allele	Phenotype*	Protruding Vulva	Blister at tip of nose	Induced by
e25	Severe ($n = 100$)	30	2	EMS (Brenner)[1]
e255	Mild ($n = 52$)	0	0	EMS (Brenner)
e324	Severe ($n = 26$)	15	0	EMS (Brenner)
e462	Mild ($n = 33$)	0	0	EMS (Brenner)
e478	Mild/Wild-type ($n = 66$)	0	0	EMS (Brenner)
ra801	Mild/Wild type ($n = 40$)	0	0	TMP (VRGCF)[2]
ra806	Mild/wild type ($n = 45$)	0	0	TMP (VRGCF)
e988	Severe/Mild ($n = 55$)	11	0	EMS (Brenner)
e1182	Mild ($n = 48$)	0	0	EMS (Brenner)
e2154	Mild/Wild-type ($n = 70$)	0	1	Mutator strain (Mancillas and Waterston, pers. Comm.)

*Based on the severity of the bent-head phenotype. The Mild designation indicates that only the tip of the nose was affected and the animals observed did not exhibit a bent-head phenotype. The Severe designation indicates that the whole head region was affected and the animals observed exhibited a bent-head phenotype.
[1]Brenner (1974) [2]Vancouver Reverse Genetics Core Facility

Basement membrane and hypodermal components associate with detached muscle cells in *unc-23* mutants.

The *unc-23* mutant phenotype reflects a defect in muscle cell attachment to the hypodermis rather than a defect in muscle cell positioning or myofilament assembly[12,13] and is seen almost exclusively in the head region even though the UNC-23 protein is present throughout the whole animal. It begins during larval development likely in response to mechanical forces exerted while the animals are foraging for food. In Unc-23 mutant worms, muscle cells detach whole from the underlying tissues. No detachment, fracturing, shearing, or separation of muscle cells from each other is observed.[12,13] A previous study by Waterston et al.[13] used electron microscopy to examine hypodermal-muscle junctions in *unc-23(e25)* mutant animals, and these authors observed delamination and local ruptures within the hypodermis. Their result indicates that the hypodermis is the site of tissue fragility and detachment in these mutants. To determine the effect of muscle cell detachment on the surrounding tissues and the location of proteins involved in attachment, both plate grown and liquid grown *unc-23(e25)* homozygous hermaphrodites were examined using antibodies that recognize components of the basement membrane or attachment structures within the hypodermis (**Fig. 5**).

UNC-52/perlecan is a basement membrane component that plays an essential role in myofilament lattice assembly.[9] This protein is distributed over the whole of the basement membrane between the body wall muscle and hypodermis and is concentrated over muscle cell dense bodies and M-lines[8] (shown in **Fig. 5A**). Examination of plate grown *unc-23(e25)* homozygous animals with the GM1 polyclonal serum[30] revealed that UNC-52/perlecan is completely absent from the areas where muscle cells have detached (see **Fig. 5B**). The distribution of UNC-52/perlecan in the rest of the animal ranges from normal to slightly disorganized in areas of stress such as the vulva. As expected, liquid grown *unc-23(e25)* mutant hermaphrodites stained with GM1 show the wild type pattern of UNC-52/perlecan localization (shown in **Fig. 5C**).

In *C. elegans,* structures called hemidesmosomes anchor the intermediate filaments within the hypodermis and are direct mediators of muscle to cuticle attachment.[8] The VAB-10/ plakin protein in the hemidesmosomal complex can be visualized by the MH5 monoclonal antibody.[17,31] In wild type animals the staining pattern of this protein appears as a series of small dots that cover the muscle quadrants with more intense staining in areas where muscle cells contact each other, but in *unc-23(e25)* homozygous animals this pattern is disrupted as was observed for perlecan (our unpublished results). Intermediate filaments are recognized by the MH4 mAb[31] and appear as repeating and equally spaced bands that run circumferentially from one edge of a muscle quadrant to the other (shown in **Fig. 5D**). Examination of MH4 staining in *unc-23(e25)* homozygous animals grown on plates revealed that there is a good deal of variability in intermediate filament organization (see **Fig. 5E**). The disruption in MH4 staining observed in affected areas can range from mild to full detachment. Homozygous *unc-23(e25)* liquid grown mutants stained with either MH5 (our unpublished data) or MH4 (**Fig. 5F**) show no disorganization or detachment and resemble wild type animals. These data show that at least some components of the basement membrane and hypodermis remain attached to the body wall muscle cells after they separate from the hypodermis. This result is consistent with the earlier conclusion of Waterston et al.[13] that the body wall muscle cells likely detach because of a weakness in the hypodermis.

Mutations in the *hsp-1* gene suppress the muscle detachment phenotype of *unc-23(e25)* mutant hermaphrodites.

We have isolated 7 independent homozygous strains that carry mutations capable of suppressing the bent head phenotype of homozygous *unc-23(e25)* hermaphrodites. All seven of these strains segregate Unc-23 mutant animals when outcrossed, and are presumed to carry unlinked suppressors of the *unc-23(e25)* mutation. The two suppressor mutations that have been characterized, *ra807* and *ra808*, are alleles of the non-inducible heat shock protein 70, *hsp-1* gene on linkage group IV.[32] Both of these mutations are dominant and fully suppress the muscle detachment phenotype of *unc-23(e25)* homozygous animals. No muscle detachment is observed in either heterozygous (*unc-23(e25); hsp-1(ra807* or *ra808)/+*)
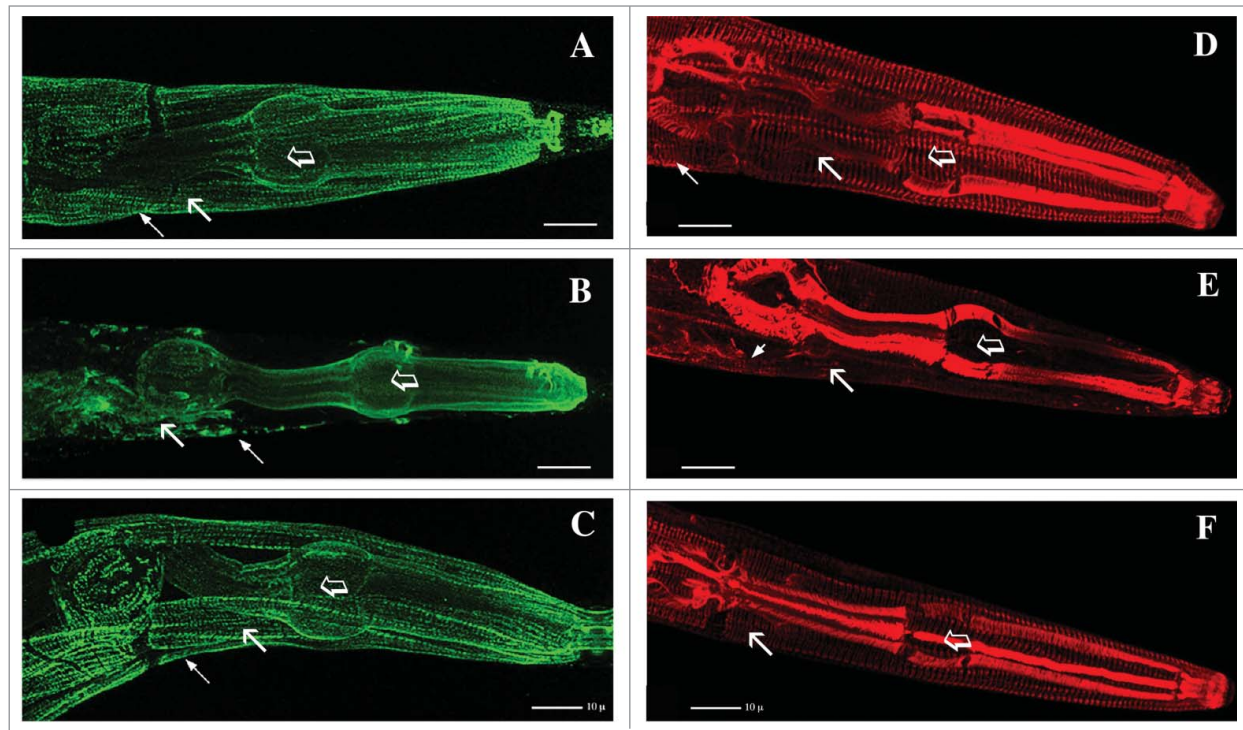
Figure 5. Wild type and *unc-23(e25)* homozygous animals are stained with antibodies against basement membrane and hemidesmosome components. Wild type hermaphrodites (**A and D**), plate grown homozygous *unc-23(e25)* adult hermaphrodites (**B and E**) and liquid grown homozygous *unc-23(e25)* adult hermaphrodites (**C and F**) stained with antibodies against UNC-52/Perlecan (**A, B and C**), and Intermediate filaments (**D, E and F**). Anterior is to the right in all panels. Scale bars are 10 microns. (**A**) A Wild type adult hermaphrodite stained with GM1, a polyclonal antibody that recognizes UNC-52/perle-can, a basement membrane proteoglycan in *C. elegans* (shown in green). The UNC-52/perlecan protein is distributed over the whole of the basement membrane and is localized to regions adjacent to the dense bodies and M lines. Note the staining of the basement membrane surrounding the pharynx. The anterior bulb of the pharynx is indicated by the open arrow-head arrow. The closed head white arrow points to a region of GM1 staining just anterior to the terminal bulb of the pharynx. (**B**) Plate grown homozygous *unc-23(e25)* adult hermaphrodite stained with GM1. The detachment and retraction of the anterior muscle cells has resulted in the detachment and disorganization of UNC-52/perlecan in the basement membrane. The closed head white arrow points to patches of UNC-52/perlecan left behind after muscle detachment. Note that in the pharynx, the organization and localization of this protein is not affected. The anterior bulb of the pharynx is indicated by the open arrow-head arrow in this image. (**C**) Liquid grown homozygous *unc-23(e25)* adult hermaphrodite stained with GM1. No evidence of disorganization or detachment is present. The anterior bulb of the pharynx is indicated by the open arrow-head arrow. The closed head white arrow points to a region of GM1 staining just anterior to the terminal bulb of the pharynx. (**D**) An adult wild type hermaphrodite stained with the MH4 monoclonal antibody which recognizes the intermediate filaments of the hypodermis (shown in red). The intermediate filaments are patterned in regularly spaced bands that extend from one edge of the muscle quadrant to the other. The closed head white arrow points to a region of MH4 staining in the hypodermis. Intermediate filaments are also present in the pharynx. The anterior bulb of the pharynx is indicated by the open arrow-head arrow. (**E**) A plate grown homozygous *unc-23(e25)* adult hermaphrodite stained with the MH4 monoclonal antibody. In these animals muscle detachment results in the disorganization and/or complete detachment of the intermediate filaments in the hypodermis. The anterior bulb of the pharynx is indicated by the open arrow-head arrow. The closed head white arrows point out the areas where intermediate filaments have detached along with the muscle cells. The organization of MH4 in the pharynx is not affected. (**F**) Homozygous *unc-23(e25)* liquid grown animals stained with the MH4 monoclonal antibody. No detachment or disorganization is observed in these animals and the intermediate filaments are found at their proper location in the hypodermis. The anterior bulb of the pharynx is indicated by the open arrow-head arrow. The closed head white arrow points to a region of MH4 staining.

or homozygous (*unc-23(e25)*; *hsp-1(ra807* or *ra808)*) suppressed animals. The remaining 5 mutations that were isolated in this screen are all recessive suppressors and have not been mapped to a chromosome.

During our genetic characterization of the suppressor strains it became apparent that hermaphrodites homozygous for either *hsp-1(ra807)* or *hsp-1(ra808)* in the *unc-23(e25)* background exhibit a temperature sensitive phenotype. These animals are healthy when grown and maintained at 15°C, but die as L3 larvae when grown at 25°C. The majority (over 95%) of the homozygous

suppressor animals either arrest development as L3 larvae or become sterile adults when grown at 20°C. When removed from the *unc-23(e25)* genetic background *hsp-1(ra807)* or *hsp-1 (ra808)* homozygous hermaphrodites appear wild type and are healthy when grown at either 15°C or 25°C. Similarly, homozygous *unc-23(e25)* hermaphrodites are viable when grown and maintained at either 15°C or 25°C. Thus, it appears that the temperature sensitive phenotype occurs only in animals homozygous for the *unc-23(e25)* mutation and either *hsp-1(ra807)* or *hsp-1(ra808)*.
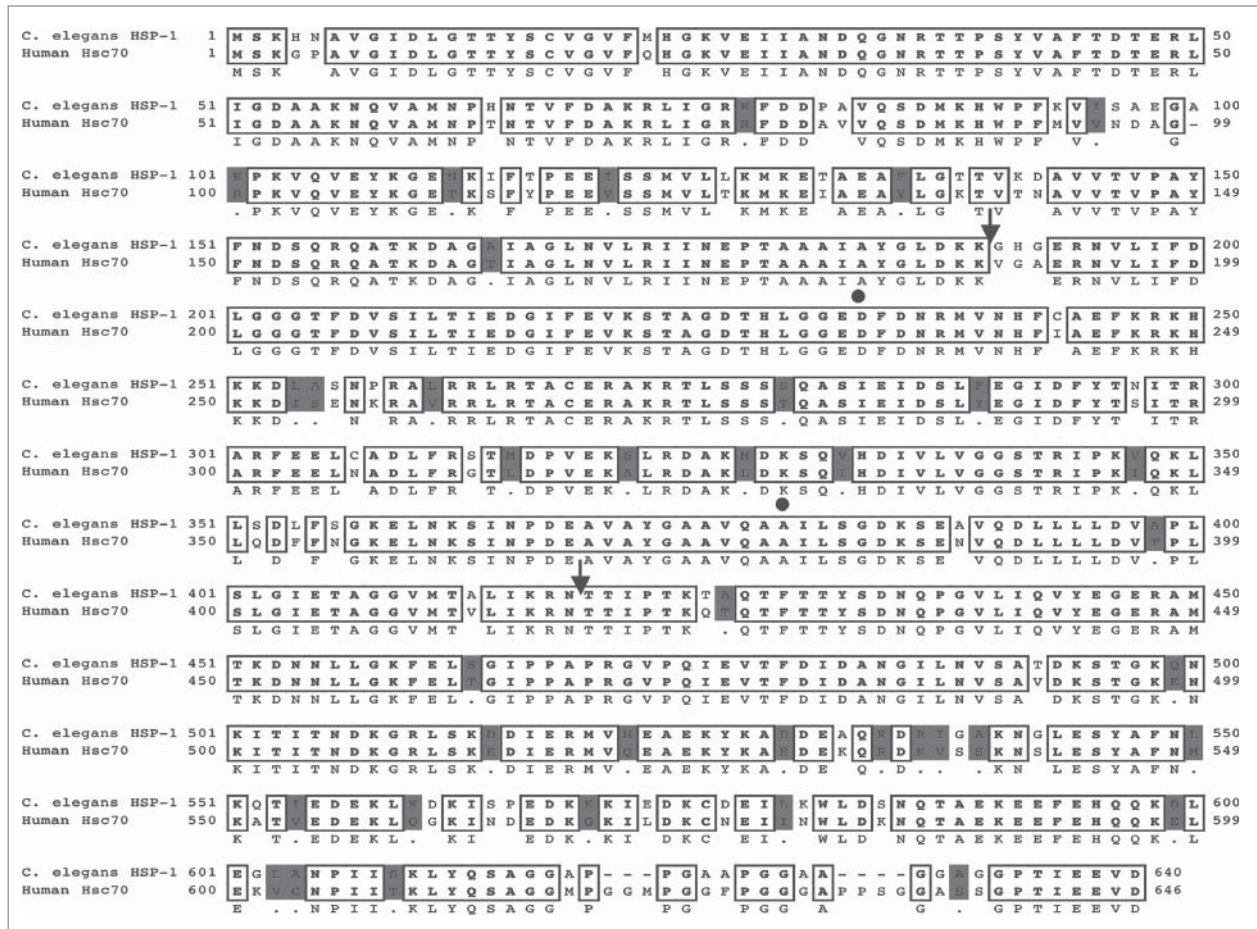
Figure 6. A comparison of the *C. elegans* HSP-1 and mammalian Hsc70 protein sequences. *C. elegans* HSP-1 and mammalian Hsc70 share 79% amino acid identity (shown as boxed residues) and 84% amino acid similarity (highlighted residues). Amino acid residues 1–386 make up the ATPase domain of the heat shock proteins. The substrate binding domain comprises residues 384 to 543, while residues 542 to 646 correspond to the variable region of the heat shock proteins. The minimal region required for UNC-23 interaction is shown by the 2 thin arrows. The amino acid residues that are altered in the *ra807* and *ra808* alleles of *hsp-1* are identified by the dots. The *ra808* mutation results in an aspartic acid to asparagine change at amino acid residue 233, and the *ra807* mutation results in an alanine to valine alteration of HSP-1 residue 379

The F26D10.3/*hsp-1* gene in *C. elegans* encodes a 640 amino acid protein with 79% identity to the mammalian Hsc70 protein[22] (**Fig. 6**; data available from GenBank/EMBL/ DDBJ under accession #Z80223). The first 386 amino acids of the HSP-1 protein comprise the ATPase domain, while amino acids 384 to 543 are involved in substrate binding. The sequence alterations corresponding to the *ra807* and *ra808* suppressor mutations have been identified and both are GC to AT point mutations that result in amino acid substitutions in the ATPase domain of the HSP-1 protein. The *ra807* mutation changes the conserved Ala379 residue to a Val residue. The *ra808* mutation replaces the conserved Asp233 residue with an Asn residue.

Suppression of the muscle detachment phenotype of *unc-23* (*e25*) by *hsp-1*(*ra807*) is allele specific. Animals homozygous for the *e324* null allele of *unc-23* still exhibit a severe bent head phenotype when either heterozygous or homozygous for the *hsp-1(ra807)* suppressor mutation. This result suggests that the *ra807* mutation does not eliminate the requirement for

HSP-1 interaction with UNC-23. Rather, the *unc-23(e25)* missense mutation, E297K, most likely results in a conformational change in the tertiary structure of UNC-23, so that its interaction with the normal HSP-1 is severely affected. The *hsp-1(ra807)* missense mutation, A379V, presumably alters the HSP-1 ATPase domain enabling it to now interact with the E297K variant of UNC-23.

The UNC-23 protein binds to the HSP-1 protein in the yeast 2-hybrid system.

The region of shared similarity between the mammalian BAG-2 protein and UNC-23 is confined to the carboxy-terminus of UNC-23 (see **Fig. 2**). Using this region of the UNC-23 protein as bait in a yeast 2-hybrid screen we identified the *hsp-1* gene product as a potential UNC-23 interacting protein. Our primary screen identified 36 clones expressing proteins that could potentially interact with the UNC-23 protein. Only ten of these showed an interaction with UNC-23 when reintroduced into

yeast and screened for a second time. When sequenced, all 10 positive clones were found to contain overlapping DNA sequences encoding the HSP-1 protein. The minimal region of the HSP-1 protein present in all of the clones extends from amino acid 189 through to amino acid 419 (see **Fig. 6**). This region is part of the ATPase domain of HSP-1 and includes the amino acids affected by the *ra807* and *ra808* suppressor mutations. Thus, our data reveal that the carboxy-terminus of UNC-23 potentially interacts with the ATPase domain of HSP-1. This result is in agreement with the mammalian results that identify BAG-2 as an Hsc70 interacting protein[24] and the more recent results demonstrating the direct interaction of these 2 nematode encoded proteins *in vitro*.[33]

Discussion

The *unc-23* gene encodes the nematode ortholog of the human BAG-2 protein, a member of the Bcl-2 associated athanogene (BAG) family of molecular chaperone regulators. In humans this protein family consists of 6 members that all contain a conserved 45 amino acid BAG domain near their C-termini, [24,25] while in *C. elegans* there are 2 members of the BAG family, UNC-23 and the F57B10.11/ *bag-1* gene product. The most intensively studied member of the human BAG family is BAG-1which was first identified as a Bcl-2 binding protein that increases the anti-apoptotic ability of cells.[34] Since its initial identification, BAG-1 has been implicated in many cellular interactions, including the binding of hepatocyte growth factor receptors ,[39] glucocorticoid receptors,[40] retinoic acid receptors,[41] and Raf-1 kinase,[42] as well as targeting to the proteasome.[39] While human BAG-1 is not known to have a role in muscle, BAG-3 has been shown to regulate filamin levels in muscle and several genetic myofibrillar myopathies have been associated with BAG-3 and filamin.[40,41]

The BAG proteins bind to and modulate the activity of the ATPase domain of the heat shock cognate protein 70, Hsc70 thus inhibiting its chaperone activity.[24,42] The protein structure of Hsc70 is conserved and can be divided into 3 functional segments, an N-terminal ATPase domain, a central substrate binding domain, and a C-terminal region that may act as a lid to the substrate-binding cleft (for a review see ref. 43). Substrate binding to Hsc70 is regulated by the binding, hydrolysis and exchange of ATP nucleotides.[45,46] The ATP bound form of Hsc70 has a low overall affinity for its substrate while the ADP bound form of Hsc70 firmly binds to its substrate. The cycling of Hsc70 between these 2 different nucleotide states is regulated by several chaperone co-factors that bind Hsc70 and modulate its ATPase activity. BAG-1 stimulates the release of ADP from the Hsc70 chaperone and, as a result, promotes the release of the bound substrate.[46-48]

Two independent *in vitro* studies on the effects of BAG-1 on Hsc70 agree that BAG-1 is probably a negative regulator of Hsc70.[47,49] BAG-1 interaction with Hsc70 *in vivo* however, can result in both inhibition and enhancement of the chaperone-dependent events, depending on which substrates are involved.[42]

This suggests that the *in vivo* function and effect of BAG-1 on Hsc70 may depend on the specific substrate and the cellular context under which the 2 proteins are interacting. Therefore, the effect of BAG-1 regulation on the chaperoning activity, chaperone-substrate complex, and the folding state of released substrate remains unclear.[42,50] Takayama et al.[24] showed that the BAG domain and the upstream region of the BAG-2 and BAG-3 proteins also interact with the ATPase domain of Hsc70 *in vitro* and *in vivo*. Some of the functional perplexity of the BAG family members may be resolved if these proteins could be studied in a model organism.

Studying the UNC-23 protein in *C. elegans* offers an opportunity to examine the possible functions of a BAG-2 ortholog within a biologically relevant context. We have shown that UNC-23 interacts with the ATPase domain of the heat shock 70 protein, HSP-1 *in vivo* and in the yeast 2-hybrid system, whereas Papsdorf et al.[33] have shown a direct interaction between these 2 proteins *in vitro* and also have demonstrated that UNC-23 acts as a nucleotide exchange factor. The results of our genetic suppression screen, which identified missense mutations in HSP-1 as suppressors of the *unc-23(e25)* muscle detachment phenotype, indicate a direct interaction between the BAG-2 homologous region of UNC-23 and HSP-1. The two dominant HSP-1 suppressor alleles, *hsp-1(ra807)* and *hsp-1(ra808)* are missense mutations that affect the ATPase domain of the protein, and are both located within the minimal region required for the yeast 2-hybrid interaction of HSP-1 with UNC-23.

Several groups have used RNA interference (RNAi) to determine the null phenotype of the *hsp-1* gene with varying results. The most severe phenotype observed was arrest during embryogenesis.[51,52] Hermaphrodites homozygous for either of the *hsp-1* suppressor alleles appear wild type in the absence of the *unc-23 (e25)* mutation suggesting they do not result in the complete loss of HSP-1 activity. Rather, they most likely alter the ATPase domain of HSP-1 allowing it to interact with the E297K mutant variant of the UNC-23/BAG-2 protein without drastically affecting its interaction with other binding partners or with the wild type UNC-23 protein.

Recently Papsdorf et al.[33] demonstrated that loss of the DNJ-13 protein in *C. elegans* acts as a suppressor of the muscle detachment induced by the loss of the UNC-23 protein. They also show that *in vitro* DNJ-13 promotes the binding of Hsc70 to its substrate while the BAG protein, UNC-23 promotes the release of Hsc70 from its substrate. Thus, DNJ-13 and UNC-23 have opposite effects on the Hsc70 chaperone and presumably HSP-1. When UNC-23 is missing but DNJ-13 is still present the system is out of balance and the muscle cells detach from the hypodermis. Apparently, in the absence of both UNC-23 and DNJ-13, the HSP-1 protein remains functional, albeit unregulated, and the muscle cells remain attached. Papsdorf et al.[33] have also found that overexpressing the *hsp-1* gene in wild type animals leads to a muscle detachment phenotype similar to that observed in Unc-23 mutant animals.

The association of UNC-23 in *C. elegans* with adhesion complexes within muscle cells and the attachment structures within the hypodermis suggests that UNC-23 acts in some manner to

regulate cell attachment and maintain hypodermal integrity. In Unc-23 mutant worms, muscle cells detach whole from the underlying tissues. No detachment, fracturing, shearing, or separation of muscle cells from each other is observed.[12,13] A previous study by Waterston et al.[13] used electron microscopy to examine hypodermal-muscle junctions in *unc-23(e25)* mutant animals, and these authors observed delamination and local ruptures within the hypodermis. Our antibody staining results revealed that the hemidesmosomes and the intermediate filament networks in the hypodermis are disrupted when muscle cells detach in *unc-23(e25)* mutant hermaphrodites. Although UNC-23 is present at the dense bodies and M lines in body wall muscle cells, no weakness or detachment is observed at these sites in detached muscle cells. In fact, restricted expression of UNC-23 to the muscle cells alone is not sufficient to rescue the bent-head phenotype of Unc-23 mutant animals (our unpublished results). Taken together these observations suggest that UNC-23 expression is required in the hypodermis to maintain the integrity of muscle cell attachments.

Based on the different phenotypes of *unc-23(e25)* homozygous animals grown in liquid or on plates, it is reasonable to predict that the interaction of UNC-23 with HSP-1 is required in biological pathways that respond to increasing contractile force by reinforcing the density and integrity of the hypodermal attachment structures. Muscle cells in liquid grown mutant hermaphrodites are capable of myofilament assembly, growth, contraction, and attachment. However, this attachment is not stable since applied external force or movement of worms on a solid substrate results in muscle detachment. Animals grown in liquid culture do not experience the shear force that plate-grown animals experience as they forage for food. Once animals are transferred to a solid substrate, they use their head muscles extensively to test the environment and forage for food. The use of the anterior muscle cells and the shear force exerted during movement initiates the muscle detachment and loss of hypodermal integrity in Unc-23 mutant hermaphrodites. This suggests that the integrity of the hypodermis is not challenged in liquid grown worms because there is less mechanical stress. The HSP-1 complex including UNC-23 and DNJ-13 must respond to cues involving mechanical stress. What those cues might be is currently unknown but may include RacGTPase, PAK-1, PIX-1 and GIT-1.[53]

New proteins may be required in response to increasing contractile force to build up existing or newly formed attachment structures in the hypodermis. HSP-1 might be involved in folding, assembling, and chaperoning these newly made proteins to their locations. Likewise, in response to an increase in contractile force, certain proteins essential for the maintenance of cell-ECM attachments might be produced in larger amounts. Hsc70 chaperones have been shown to interact with several cytoskeletal proteins including intermediate filaments[54,55] and microtubules.[54-57] Production of large amounts of intermediate filaments, for example, would be required at newly made hypodermal attachment sites and for the reinforcement of existing attachment structures to help maintain the integrity of the hypodermis. HSP-1 might bind the intermediate filaments to prevent their aggregation and chaperone them to their proper location.

The chaperone functions of HSP-1 are not limited to interaction with intermediate filaments. Membrane bound receptors and structural proteins that make up the attachment structures and/ or bind the intermediate filaments are other possible substrates for HSP-1. If UNC-23 functions as a negative regulator of HSP-1, in the same manner as BAG-2, then one might predict that the interaction of UNC-23 with HSP-1 is required for the release of the substrate from the binding cleft of HSP-1. In the absence of UNC-23, HSP-1 is unable to release its substrate in response to mechanical stresses experienced by the hypodermis. The subcellular localization of UNC-23 in the hypodermis is pertinent to this type of model, since its distribution is reminiscent of the distribution of the intermediate filaments within the hypodermis. The predicted role of UNC-23 as a regulator that promotes HSP-1 substrate release, agrees with the localization pattern observed in the hypodermis.

It is important to note that the UNC-23/HSP-1 interaction is not necessary for the initial assembly and localization of attachment structures during embryogenesis, or for the maintenance of attachment structures within the body wall muscle cells. Given the number of biological pathways that HSP-1 is involved it is not surprising that loss of *hsp-1* gene function by RNA interference results in embryonic lethality.[51,52] Mutations in the *unc-23* gene do not result in a similar phenotype; they only affect the hypodermal integrity and muscle cell attachment of the anterior body wall muscle cells. This suggests that the interaction of UNC-23 with HSP-1 provides specificity for HSP-1 function to the biological pathway(s) in the hypodermis that are involved in the maintenance of muscle attachment during development. UNC-23 as a chaperone regulator thus refines the amount of proteins deposited at adhesions junctions in developing and growing *C. elegans* animals.

Materials and Methods

Nematode strains

The *unc-23* mutant strains used in this study were provided by Jonathan Hodgkin at the MRC-LMB (Cambridge, England), the *Caenorhabditis* Genetics Center (CGC) at the University of Minnesota (Minneapolis, Minnesota), the *C. elegans* Reverse Genetics Core Facility at the University of British Columbia (Vancouver, British Columbia), and Edward Hedgecock at Johns Hopkins University (Baltimore, Maryland). Strains carrying the *sDf71* and *mDf1* deficiencies were obtained from David Baillie at Simon Fraser University (Burnaby, British Columbia). Strains carrying the ZC196, B0507, C01B7, W09B7, ZC411, K06C4, H14N18, T19A5, F59E11 and R03H4 cosmids were kindly provided by Michael Nonet at Washington University School of Medicine (St. Louis, Missouri). The DM5110: *sDf71/ dpy-11(e224)*V and DM5111: *mDf1/ dpy-11(e224)*V strains were constructed for this study.

Growth in liquid culture

Worms were grown in liquid culture in 250 ml flasks containing 50 ml 5% (W/V) OP50 in S medium at 20°C and aerated by

shaking at 200 rpm. Adult animals were washed from plates, then transferred to liquid culture and allowed to grow for at least one generation. The liquid grown animals were spun gently in glass tubes to remove the culture medium and then washed twice in M9 buffer before antibody staining. Hermaphrodites for polarized light microscopy were grown in micro-titer wells containing 150 ml of 5% (W/V) *E. coli* X1666 in S medium. Two adult animals were placed in each well. The adult F1or F2 progeny were removed from the wells with a pipette, placed on a plate and then transferred to 11.5 ml of M-9 buffer on a glass slide.

Mapping deficiency breakpoints by PCR

The following PCR strategy was used to determine if a particular cosmid was deleted by either *sDf71* or *mDf1*. Arrested embryos homozygous for the deficiency were treated with proteinase K, and the DNA obtained was used in PCR reactions as previously described.[53] The genomic sequence of the cosmids in the region of *unc-23* was obtained from the *Caenorhabditis elegans* Genome Sequencing Consortium,[22] and a series of primers were designed that would amplify specific DNA fragments from these cosmids. If a fragment of the correct size was amplified using DNA isolated from the arrested mutants, then that region of the cosmid was not deleted by the deficiency. If the correct fragment was not obtained then the region covered by the primers was deleted by the deficiency. Approximately 4–6 arrested *sDf71* or *mDf1* homozygous embryos, obtained from the DM5110 and DM5111 strains, were used per PCR reaction. Polymorphisms associated with particular *unc-23* mutations were identified in a similar manner using primer sets designed to amplify the H14N18.1 ORF.

Sequence analysis of *unc-23* and *hsp-1*

The Nucleic Acid/Protein Service (NAPS) unit at the University of British Columbia did all of the sequencing for this study. The full-length *unc-23* cDNA, YK293b4 was obtained as a λZapII clone from the *C. elegans* cDNA project (kindly provided by Dr. Y. Kohara, National Institute of Genetics, Mishima, Japan). The bluescript plasmid containing the cDNA insert was excised and transformed into XL1 blue cells following the protocol provided by Stratagene (PDI Bioscience Inc.., Aurora, Ontario). Plasmid DNA was prepared for sequencing using the Qiagen miniprep kit (catalog # 27106. QIAGEN Inc. Mississauga, Ontario). The entire cDNA insert was sequenced to independently confirm the exon/intron boundaries predicted by the Genefinder program.

Three overlapping DNA fragments were amplified from mutant hermaphrodites homozygous for the *e25, e324, e988, ra801, ra806,* and *rh192* alleles of *unc-23* using the polymerase chain reaction as described by Rogalski et al.[58] The 3 primer sets used cover all of exons 2, 3, 4, and the majority of exon 5 (except for the last 25 bps) of the H14N18.1/ *unc-23* gene. Overlapping DNA fragments that span the whole of the *hsp-1* gene were amplified from adult hermaphrodites homozygous for the *hsp-1 (ra807)* and *hsp-1(ra808)* mutations. All PCR fragments were prepared for sequencing using the QIAquick PCR purification Kit (Catalog #28104. QIAGEN Inc. Mississauga, Ontario).

Proteins with sequence similarity to UNC-23 were identified using the NCBI blast search algorithm.[59] The Clustal W program (MacVector 6.0, Oxford Molecular Group) was used for protein sequence alignment and comparison.

Immunofluorescence staining and microscopy

Adult hermaphrodites were stained as described by Finney and Ruvkin[60] with some minor modifications. Incubation times were overnight at 15°C for both the primary and secondary antibodies. The mouse monoclonal antibodies MH4 and MH5[31] were diluted 1:200, while the rabbit polyclonal sera GM1[61] was diluted 1:50. The secondary antibodies, FITC-labeled donkey anti-mouse IgG F(ab')$_2$ and TRSC-labeled donkey anti-rabbit IgG F(ab')$_2$ (Jackson ImmunoReseach Laboratories; West Grove, PA, USA) were diluted 1:200.

Confocal images were captured on a BioRad MRC 600 system, using the CoMOS 7.0a application. Optical sections of adult worms were collected at 0.2μ intervals (Z steps) for the full depth of the specimen. Z-series were imported to NIH image 1.60 for viewing and projections. For final images, projections were imported into Adobe Photoshop (Versions 5.0 and 7.0).

Worms examined under polarized light were removed from NGM plates, placed in a drop of M9 buffer on a slide, and then immobilized by placing a coverslip over them. Polarized microscopy was done on a Zeiss Axiophot Photomicroscope (Carl Zeiss D-7082 Oberkochen).

Construction of DNA fragments for microinjection

A DNA fragment containing the *unc-23* promoter and coding region (minus the TAG stop codon) fused to the green fluorescent protein (GFP) was constructed using the technique described by Cassata et al.[62] and Hobert et al.[28] The GFP coding and 3' untranslated sequences were derived from the pPD95.75 (Fire LabVector Kit available at http://www.addgene.org/pgvec1? f=c andcmd=showcol andcolid=1). The *unc-23* promoter that was used starts at -2166 upstream of the ATG start codon. This region contains all of the 5' upstream region of the *unc-23* gene plus a portion of the 3' UTR of the upstream H14N18.2 gene The DNA fragments obtained were purified for microinjection using the QIAquick PCR purification Kit (Cat. # 28104. QIAGEN Inc. Mississauga, Ontario).

Microinjections of *C. elegans*

Microinjections of adult hermaphrodites were performed as described by Mello and Fire.[63] The *unc-23*::GFP DNA fragment (∼10ηg/μl) was co-injected with the pPD95.75 GFP plasmid (∼33ηg/μl) and the pRF#4 *rol-6* plasmid (∼78ηg/μl) into the gonad syncytium of wild type hermaphrodites. The pPD95.75 GFP plasmid was included in the injection mix because it has homology to the *unc-23*::GFP PCR fragment. F1 Rol hermaphrodites were selected and any that produced Rol progeny were kept as transgenic strains. The following transgenic strain was obtained: DM7020: +/+; *raEx20*[pRF#4{*rol-6(su1006dm)*} + *unc-23*::GFP + pPD95.75(GFP)].

Strains homozygous for *unc-23(e25)* and carrying the *raEx20* array were constructed by mating +/+; *raEx* Rol hermaphrodites with *unc-23(e25)* / + males. Single F1 Rol hermaphrodites with

the genotype *unc-23(e25)* / +; *raEx20* were selected and Rol hermaphrodites that were homozygous *unc-23(e25)* were obtained from among the progeny of these animals

Isolation and mapping of suppressor mutations of *unc-23 (e25)*

Mutagenesis was done using 0.05 M ethyl methanesulfonate (EMS) in M9 buffer as described by Sulston and Hodgkin.[64] Dominant and recessive revertants were obtained by screening both the F1 and F2 progeny of approximately 1000 mutagenized *unc-23(e25)* homozygous hermaphrodites for well-moving animals that lacked the bent-head phenotype. Individual wild type worms were transferred to new plates and their progeny were screened for the presence of the Unc-23 and wild type phenotypes. Homozygous suppressor strains were established by picking wild type animals that failed to segregate Unc-23 progeny. All of the strains obtained segregated Unc-23 animals in the F2 generation after outcrossing to wild type males, indicating that the suppressor mutations were not closely linked to the *unc-23* gene.

The *ra807* and *ra808* suppressor alleles were mapped to linkage group IV in the following manner. Males of genotype *unc-23 (e25)* / + V; *dpy-13(e184)* /+ IV were mated with homozygous suppressors hermaphrodites (*unc-23(e25)*V; *hsp-1(ra807or8)*IV). F1 progeny with the genotype *unc-23(e25)*V; *dpy-13(e184)* + /+ *hsp-1(ra807or8)*IV were selected and allowed to reproduce. In the case of the *ra807* and *ra808* dominant suppressor mutations only Wild and DpyUnc F2 progeny were observed. The absence of Dpy nonUnc and Unc nonDpy F2 progeny indicated that the suppressor mutations were linked to *dpy-13(e184)* IV. The recessive suppressor mutations have not been mapped.

The *hsp-1(ra807)* IV; *unc-23*(e324)V strain was constructed by mating *unc-23(e324)* / + V; GFP(*cv24*) IV males with *hsp-1 (ra807)*IV; *dpy-11(e224)*V hermaphrodites. Progeny with the genotype GFP(*cv24*) + / + *hsp-1(ra807)*IV; *unc-23(e324)* / *dpy-11(e224)*V were identified and allowed to reproduce. The presence of Unc nonGFP hermaphrodites (genotype: *hsp-1(ra807)* IV; *unc-23(e324)*V) indicated that the *e324* allele of *unc-23* is not suppressed by the *hsp-1(ra807)* mutation.

Construction of clones for yeast 2-hybrid screens

The pDM#220 (pGBDU-C3 + *unc-23* bait) and pDM#221 (pGAD-C3 + *unc-23* bait) plasmid clones were constructed as follows. A 614 bp DNA fragment was amplified from an *unc-23* cDNA clone using the PWO DNA Polymerase kit (Roche Molecular Biochemicals, Catalog #1644 947. Mannheim, Germany), inserted into a pCR-BLUNT vector (Invitrogen, Carlsbad, California) as described by the manufacturer (http://www.invitrogen.com) and transformed into DH5α competent cells (Life Technologies, catalog #18265–017. Burlington, Ontario). The *unc-23* encoding DNA fragment was released from the pCR-BLUNT vector and re-inserted into the Eco RI sites of the pGBDU-C3 and pGAD-C3 vectors.[65] The orientation and

sequence of the cloned *unc-23* encoding DNA fragments were determined by PCR analysis and sequencing. The yeast strain PJ69–4A was transformed with the pDM#220 and pDM#221 clones as described by James et al.[65] to obtain the yDM#220 and yDM#221 yeast strains.

The yDM#220 strain was used as the bait to screen a mixed stage *C. elegans* cDNA yeast 2-hybrid library (kindly provided by Bob Barstead, Oklahoma Medical Research Foundation, Oklahoma City, OK) as described by James et al.[65] Briefly, colonies obtained on His⁻ selection plates were transferred to adenine minus (Ade⁻) plates to be re-screened for their positive interaction. The established colonies on Ade⁻ plates were transferred to a third selection plate containing 5-Fluoroorotic Acid (FOA) to promote loss of the bait plasmid. The prey plasmid was recovered and re-transformed into yDM#220 cells to confirm the initial positive interaction. DNA was isolated from the plasmids that showed an interaction with yDM#220 and sequenced by the NAPS unit at the University of British Columbia.

Authors' Contributions

Conceived and designed experiments: PR, DM. Performed the experiments: PR, TR. Analyzed the data: PR, TR, DM. Wrote the paper: PR, TR, DM.

References

1. Chin-Sang ID, Chisholm AD. Form of the worm: genetics of epidermal morphogenesis in *C. elegans*. Trends Genet 2000; 16:544-551; PMID:11102704

2. Beloussov LV, Dorfman JG, Cherdantzev VG. Mechanical stresses and morphological patterns in amphibian embryos. J Embryol Exp Morphol 1975; 34:559-574.

3. Nance J, Lee JY, Goldstein B. Gastrulation in *C. elegans*. WormBook; 2005:1-13; doi:10.1895/wormbook.1.23.1, http://www.wormbook.org.

4. Hay E. 1992. Cell biology of extracellular matrix, 2nd edition. Plenum Press, New York.

5. Wang J H-C, Thampatty BP, Lin J-S, Im H-J. Mechanoregulaton of gene expression in fibroblasts. Gene 2007; 1:1-15; PMID:17331678

6. Ingber DE. Tensegrity: the architectural basis of cellular menchanotransduction. Annu Rev Physiol 1997; 59:575-99; PMID:9074778

7. Fuchs E, Cleveland DW. A structural scaffolding of intermediate filaments in health and disease. Science 1998; 279:514-519; PMID:9438837

8. Francis R, Waterston RH. Muscle cell attachment in *Caenorhabditis elegans*. J Cell Biol 1991; 114:465-479; PMID:1860880

9. Rogalski TM, Williams BD, Mullen GP, Moerman DG. Products of the unc-52 gene in *Caenorhabditis elegans* are homologous to the core protein of the mammalian basement membrane heparan sulfate proteoglycan. Genes Dev 1993; 7:1471-1784; PMID:8393416

10. Kramer JM. 1997 C. elegans II. Editors: Riddle DL, Blumenthal T, Meyer BJ, Priess JR. Cold Spring Harbor Laboratory Press. New York. Pages 471-500.

11. Hresko MC, Williams BD, Waterston RH. Assembly of body wall muscle and muscle cell attachment structures in *Caenorhabditis elegans*. J Cell Biol 1994; 124:491-506; PMID:8106548

12. Plenefisch JD, Zhu X, Hedgecock EM. Fragile skeletal muscle attachments in dystrophic mutants of *Caenorhabditis elegans*: isolation and characterization of the mua genes. Development 2000; 127:1197-1207; PMID:10683173

13. Waterston RH, Thomson JN, Brenner S. Mutants with altered muscle structure in *Caenorhabditis elegans*. Dev Biol 1980; 77:271-302; PMID:7190524

14. Hresko MC, Schriefer LA, Shrimankar P, Waterston RH. Myotactin, a novel hypodermal protein involved in muscle-cell adhesion in *Caenorhabditis elegans*. J Cell Biol 1999; 146:659-672; PMID:10444073

15. Bercher M, Wahl J, Vogel BE, Lu C, Hedgecock EM, Hall DH, Plenefisch JD. mua-3, a gene required for mechanical tissue integrity in *Caenorhabditis elegans*, encodes a novel transmembrane protein of epithelial attachment complexes. J Cell Biol 2001; 154:415-426; PMID:11470828

16. Hapiak V, Hresko MC, Schriefer LA, Saiyasisongkhram K, Bercher M, Plenefisch J. mua-6, a gene required for tissue integrity in *Caenorhabditis elegans*, encodes a cytoplasmic intermediate filament. Dev Biol; 2003 263:330-342; PMID:14597206

17. Bosher JM, Hahn BS, Legouis R, Sookhareea S, Weimer RM, Gansmuller A, Chisholm AD, Rose AM, Bessereau JL, Labouesse M. The *Caenorhabditis elegans* vab-10 spectraplakin isoforms protect the epidermis against internal and external forces. J Cell Biol 2003; 161:757-768; PMID:12756232

18. Hong L, Elbl T, Ward J, Franzini-Armstrong C, Rybicka KK, Gatewood BK, Baillie DL, Bucher EA. MUP-4 is a novel transmembrane protein with functions in epithelial cell adhesions in *Caenorhabditis elegans*. J Cell Biol 2001; 154:403-414; PMID:11470827; http://dx.doi.org/10.1083/jcb.200007075

19. Woo WM, Goncharov A, Jin Y, Chisholm AD. Intermediate filaments are required for *C. elegans* epidermal elongation. Dev Biol 2004; 267:216-229; PMID:14975728; http://dx.doi.org/10.1016/j.ydbio.2003.11.007

20. Hetherington S, Gally C, Fritz JA, Polanowska J, Reboul J, Schwab Y, Zahreddine H, Behm C, Labouesse M. PAT-12, a potential anti-nematode target, is a new SpectraPlakin partner essential for *Caenorhabditis elegans* hemidesmosomal integrity and embryonic morphogenesis. Dev Biol 2011; 350:267-278; PMID:21130760; http://dx.doi.org/10.1016/j.ydbio.2010.11.025

21. Brenner S. The genetics of *Caenorhabditis elegans*. Genetics 1974; 77:71-94; PMID:4366476

22. C. elegans Sequencing Consortium. Genome sequence of the nematode *C. elegans*: a platform for investigative biology. Science 1998; 282:2012-2018; PMID:9851916; http://dx.doi.org/10.1126/science.282.5396.2012.

23. Eckman FH, Durbin R. ACeDB and Macace. In *Caenorhabditis elegans*: modern biological analysis of an organism. Editors: HF Epstien, DC Shakes. Academic press, San Diego. 1995:Pages 586-605.

24. Takayama S, Xie Z, Reed JC. An evolutionary conserved family of Hsp70/Hsc70 molecular chaperone regulators. J Biol Chem 1999; 274:781-786; PMID:9873016; http://dx.doi.org/10.1074/jbc.274.2.781

25. Kabbage M, Dickman MB. The Bag proteins: a ubiquitous family of chaperone regulators. Cell Mol Life Sci 2008; 65:1390-1402; PMID:18264803; http://dx.doi.org/10.1007/s00018-008-7535-2

26. Gettner SN, Kenyon C, Reichardt L. Characterization of bpat-3 heterodimers, a family of essential integrin receptors in *C. elegans*. J Cell Biol 1995; 129:1127-1141; PMID:7744961; http://dx.doi.org/10.1083/jcb.129.4.1127

27. Rogalski TM, Mullen GP, Gilbert MM, Williams BD, Moerman DG. The UNC-112 gene in *Caenorhabditis elegans* encodes a novel component of cell-matrix adhesion structures required for integrin localization in the muscle cell membrane. J Cell Biol 2000; 150:253-264; PMID:10893272; http://dx.doi.org/10.1083/jcb.150.1.253

28. Hobert O, Moerman DG, Clark KA, Beckerle MC, Ruvkun G. A conserved LIM protein that affects muscular adherens junction integrity and mechanosensory function in *Caenorhabditis elegans*. J Cell Biol 1999; 144:45-57; PMID:9885243; http://dx.doi.org/10.1083/jcb.144.1.45

29. Mackinnon AC, Qadota H, Norman KR, Moerman DG, Williams BD. *C. elegans* PAT-4/ILK functions as an adaptor protein within integrin adhesion complexes. Curr Biol 2002; 12:787-797; http://dx.doi.org/10.1016/S0960-9822(02)00810-2

30. Mullen GP, Rogalski TM, Bush JA, Rahmani Gorji P, Moerman DG. Complex pattern of alternative splicing mediate the spatial and temporal distribution of perlecan/UNC-52 in *Caenorhabditis elegans*. Mol Biol Cell 1999; 10:3205-3221; PMID:10512861; http://dx.doi.org/10.1091/mbc.10.10.3205

31. Francis R, Waterston RH. Muscle organization in *Caenorhabditis elegans*: localization of proteins implicated in thin filament attachment and I band organization. J Cell Biol 1985; 101:1532-1549; PMID:2413045; http://dx.doi.org/10.1083/jcb.101.4.1532

32. Snutch TP, Heschl MF, Baillie DL. The *Caenorhabditis elegans* hsp70 gene family: a molecular genetic characterization. Gene 1988; 64:241-255; PMID:2841196; http://dx.doi.org/10.1016/0378-1119(88)90339-3

33. Papsdorf K, Sacherl J, Richter K. The balanced regulation of Hsc70 by DNJ-13 and UNC-23 is required for muscle functionality. J Biol Chem 2014; 289:252250-252261; http://dx.doi.org/10.1074/jbc.M114.565234

34. Takayama S, Sato T, Krajewski S, Kochel K, Irie S, Millan JA, Reed JC. Cloning and functional analysis of BAG-1: A novel Bcl-2-binding protein with anti-cell death activity. Cell 1995; 80:279-284; PMID:7834747; http://dx.doi.org/10.1016/0092-8674(95)90410-7

35. Bardelli A, Longati P, Albero D, Goruppi S, Schneider C, Ponzetto C, Comoglio PM. HGF receptor associates with the anti-apoptotic protein BAG-1 and prevents cell death. EMBO J 1996; 15:6205-6212; PMID:8947043

36. Kanelakis KC, Morishima Y, Dittmar KD, Galigniana MD, Takayama S, Reed JC, Pratt WB. Differential effects of the hsp70-binding protein BAG-1 on glucocorticoid receptor folding by the hsp90-based chaperone machinery. J Biol Chem 1999; 274:34134-34140; PMID:10567384; http://dx.doi.org/10.1074/jbc.274.48.34134

37. Liu R, Takayama S, Zheng Y, Froesch B, Chen G, Zhang X, Reed JC, Zhang X. Interaction of BAG-1 with retinoic acid receptor and its inhibition of retinoic acid-induced apoptosis in cancer cells. J Biol Chem 1998; 273:16985-16992; PMID:9642262; http://dx.doi.org/10.1074/jbc.273.27.16985

38. Wang H, Takayama S, Rapp UR, Reed JC. Bcl-2 interacting protein, BAG-1, binds to and activates the kinase Raf-1. Proc Natl Acad Sci USA 1996; 93:7063-7068; http://dx.doi.org/10.1073/pnas.93.14.7063

39. Luders J, Demand J, Hohfeld J. The ubiquitin-related BAG-1 provide a link between the molecular chaperones Hsc70/Hsp70 and the proteasome. J Biol Chem 2000; 275:4613-4617; PMID:10671488; http://dx.doi.org/10.1074/jbc.275.7.4613

40. Ulbricht A, Eppler FJ, Tapia VE, van der Ven PFM, Hampe N, Hersch N, Vakeel P, Stadel D, Haas A, Saftig P, et al. Cellular mechanotransduction relies on tension-induced and chaperone-assisted autophagy. Curr Biol 2013; 23:430-5; http://dx.doi.org/10.1016/j.cub.2013.01.064

41. Vorgerd M, van der Ven PFM, Bruchertseifer V, Löwe T, Kley Ra, Schröder R, Lochmüller H, Himmel M, Koehler K, Fürst DO, et al. A mutation in the dimerization domain of filamin c causes a novel type of autosomal dominant myofibrillar myopathy. Am J Hum Genet 2005; 77:297-304; PMID:15929027; http://dx.doi.org/10.1086/431959

42. Takayama S, Bimston DN, Matsuzawa S, Freeman BC, Aime-Sempe C, Xie Z, Morimoto R, Reed JC. BAG-1 modulates the chaperone activity of Hsp70/Hsc70. EMBO J 1997; 16:4887-4896; PMID:9305631; http://dx.doi.org/10.1093/emboj/16.16.4887

43. Doong J, Vrailas A, Kohn C. What's in the BAG? – A functional domain analysis of the BAG-family proteins. Cancer Lett 2002; 188:25-32; http://dx.doi.org/10.1016/S0304-3835(02)00456-1

44. McCarty JS, buchberger A, Reinstein J, Bukau B. The role of the ATP in functional cycle of the DnaK chaperone system. J Mol Biol 1995; 249:126-137; PMID:7776367; http://dx.doi.org/10.1006/jmbi.1995.0284

45. Rudiger S, Buchberger A, Bukau B. Interaction of Hsp70 chaperones with substrates. Nat Struct Biol 1997; 4:342-349; PMID:9145101; http://dx.doi.org/10.1038/nsb0597-342

46. Hohfeld J, Jentsch S. Grp-E-like regulation of the Hsc70 chaperone by the antiapoptotic protein BAG-1. EMBO J 1997; 16:6209-6216; PMID:9321400; http://dx.doi.org/10.1093/emboj/16.20.6209

47. Nollen EAA, Brunsting JF, Song J, Kampinga HH, Morimoto RI. Bag-1 functions in vivo as a negative regulator of Hsp70 chaperone activity. Mol Cell Biol 2000; 20:1083-1088; PMID:10629065; http://dx.doi.org/10.1128/MCB.20.3.1083-1088.2000

48. Nollen EAA, Kabakov AE, Brunsting JF, kanon B, Hohfeld J, Kampinga HH. Modulation of in vivo HSP70 chaperone activity by Hip and BAG-1. J Biol Chem 2001; 276:4677-4682; PMID:11076956; http://dx.doi.org/10.1074/jbc.M009745200

49. Bimston D, Song J, Winchester D, Takayama S, Reed JC, Morimoto RI. BAG-1, a negative regulator of Hsp70 chaperone activity, uncouples nucleotide hydrolysis from substrate release. EMBO J 1998; 17:6871-6878; PMID:9843493; http://dx.doi.org/10.1093/emboj/17.23.6871

50. Hohfeld J. Regulation of the heat shock cognate Hsc71 in the mammalian cell: the characterization of the anti-apoptotic protein BAG-1 provides novel insight. Biol Chem 1998; 379:269-274; PMID:9563821

51. Piano F, Schetter AJ, Mangone M, Stein L, Kemphues KJ. RNAi analysis of genes expressed in the ovary of *Caenorhabditis elegans*. Curr Biol 2000; 28:1619-1622; http://dx.doi.org/10.1016/S0960-9822(00)00869-1

52. Rual JF, Ceron J, Koreth J, Hao T, Nicot AS, Hiro-zane-Kishikawa T, Vandenhaute J, Orkin SH, Hill DE, van den Heuvel S, Vida lM. Toward improving Caenorhabditis elegans phenome mapping with an ORFeome-based RNAi library. Genome Res 2004; 14:2162-2168; PMID:15489339; http://dx.doi.org/10.1101/gr.2505604

53. Zhang H, Landmann F, Zahreddine H, Rodriguez D, Koch M, Labouesse M. A tension-induced mechano-transduction pathway promotes epithelial morphogenesis. Nature 2011; 471:99-103; PMID:21368832; http://dx.doi.org/10.1038/nature09765

54. Napolitano EW, Pachter JS, Chin SS, Liem RK. β-Internexin, a ubiquitous intermediate filament-associated protein. J Cell Biol 1985; 101:1323-1331; PMID:3900089; http://dx.doi.org/10.1083/jcb.101.4.1323

55. Liao J, Lowthert LA, Ghori N, Omary MB. The 70-kDa heat shock proteins associate with glandular intermediate filaments in an ATP-dependent manner. J Biol Chem 1995; 270:915-922; PMID:7529764; http://dx.doi.org/10.1074/jbc.270.2.915

56. Ohtsuka K, Tanabe K, Nakamura H, Sato C. Possible cytoskeletal association of 69,000- and 68,000-dalton heat shock proteins and structural relations among heat shock proteins in murine mastocytoma cells. Radial Res 1986; 108:34-42; http://dx.doi.org/10.2307/3576967

57. Green LA, Liem RK. Beta-internexin is a microtubule-associated protein identical to the 70-kDa heat-shock cognate protein and the clathrin uncoating ATPase. J Biol Chem 1989; 264:15210-15215; PMID:2527848

58. Rogalski TM, Gilchrist EJ, Mullen GP, Moerman DG. Mutations in the unc-52 gene responsible for body wall muscle defects in adult *Caenorhabditis elegans* are located in alternatively spliced exons. Genetics 1995; 139:159-169; PMID:7535716

59. Altschul SF, Madden TL, Schäffer AA, Zhang J, Zhang Z, Miller W, Lipman DJ. Gapped BLAST and PSI-BLAST: a new generation of protein database search programs. Nucleic Acids Res 1997; 25:3389-402; PMID:9254694; http://dx.doi.org/10.1093/nar/25.17.3389

60. Finney M, GB Ruvkun. The unc-86 gene product couples cell lineage and cell identity in *C. elegans*. Cell 1990; 63:895-900; PMID:2257628; http://dx.doi.org/10.1016/0092-8674(90)90493-X

61. Moerman DG, Hutter H, Mullen GP, Schnabel R. Cell autonomous expression of perlecan and plasticity of cell shape in embryonic muscle of *Caenorhabditis elegans*. Dev Biol 1996; 173:228-242; PMID:8575624; http://dx.doi.org/10.1006/dbio.1996.0019

62. Cassata G, Kagoshima H, Prétôt RF, Aspöck G, Niklaus G, Bürglin TR. Rapid expression screening of *Caenorhabditis elegans* homeobox open reading frames using a two-step polymerase chain reaction promoter-gfp reporter construction technique. Gene 1998; 212:127-135; PMID:9661672; http://dx.doi.org/10.1016/S0378-1119(98)00137-1

63. Mello C, Fire A. DNA transformation. Methods Cell Biol 1995; 48:451-482; PMID:8531738; http://dx.doi.org/10.1016/S0091-679X(08)61399-0

64. Sulston JE, Hodgkin J. 1988. Methods. In The nematode Caenorhabditis elegans. Editor WB Wood and the community of *C. elegans* researchers. Cold Spring Harbor Laboratory, Cold Spring Harbor, New York

65. James P, Halladay J, Craig EA. Genomic libraries and host strain designed for highly efficient two-hybrid selection in yeast. Genetics 1996; 144:1425-1436; PMID:8978031